



Synthesis, morphology and spectroscopy of Nd:GSAG nano-powders

Jing Su*, Yijun Yao, Bin Liu, Linhua Xu

School of Physics and Optoelectronic Engineering, Nanjing University of Information Science and Technology, Nanjing 210044, China

ARTICLE INFO

Article history:

Received 18 December 2011
Received in revised form 27 January 2012
Accepted 5 February 2012
Available online xxx

Keywords:

Chemical synthesis
Phase transitions
Optical spectroscopy
Luminescence

ABSTRACT

Nd³⁺-doped gadolinium scandium aluminum garnet (Nd:GSAG) precursors were obtained from a mixed nitrate solution with precipitant of ammonium hydrogen carbonate. The precursors were sintered at different temperatures and the phase developments in heat treatments were investigated through methods of XRD and IR, showing the precursors transformed to pure-GSAG phase with no intermediate phases appeared at 900 °C. The TEM observation revealed that the powders sintered at 900–1000 °C were well-dispersed with average crystalline sizes of 30–80 nm. Photoluminescence analysis of the Nd:GSAG nano-powders showed that the PL intensities changing significantly with the Nd³⁺ doping concentration, and the concentration quenching was observed as the Nd³⁺ concentration reached to 1.5 at.%.
© 2012 Elsevier B.V. All rights reserved.

1. Introduction

The special wavelength regions around 940 nm have been specified to be a space-borne differential absorption LIDAR (DIAL) for atmospheric water vapor detection [1,2]. Although the laser outputs at these wavelengths can be easily obtained by conventional ways of optical parametric oscillator (OPO), Ti:Sapphire laser generation and Raman-shifter, they exhibit many disadvantages, such as low efficiency and complex set-up. To solve these problems, development for suitable laser crystals pumped by laser diode (LD) has become a good choice and attracted wide interests. Being a type of crystals that can generate LD pumped 940 nm laser output, the garnet crystals, such as Nd³⁺-doped gadolinium scandium aluminum garnet (Nd:GSAG) single crystal, have achieved a great development [3,4]. However, as a traditional laser material, single crystal has shown some disadvantages, such as the difficulties in grow large-size, uniform and high rare earth ion-doped crystal for the limitation of crystal growth technique. Recently, the transparent laser ceramics seem to be an alternative replacement for laser crystals. Since the first Nd³⁺-doped yttrium aluminum garnet (Nd:YAG) ceramic laser was developed in 1995 [5], the advantages of transparent ceramics, such as fabrication of large size and high doping concentration, low price, ease of manufacture and mass production, have attracted great interests to develop this potential laser material [6–8]. Although, to our knowledge, few results reported on the Nd:GSAG transparent ceramics had been found. For fabrication of Nd:GSAG transparent ceramics with

high-performance, well-sinterable Nd:GSAG powders are necessary. In this work, Nd:GSAG nano-powders were prepared via co-precipitation. Phase transition of the precursors, morphology and luminescence of Nd:GSAG powders were investigated.

2. Methods

Gd(NO₃)₃, Sc(NO₃)₃ and Nd(NO₃)₃ solution were prepared by dissolving Gd₂O₃, Sc₂O₃, Nd₂O₃ with purity of 99.995% into diluted HNO₃. Al(NO₃)₃ solution was obtained by dissolving Al(NO₃)₃·9H₂O (>99%) in de-ionized water. Nitrate solutions were mixed according to the molar ratio of (Gd_{1-x}Nd_x)₃Sc₂Al₃O₁₂ (x = 0.01, 0.015, 0.02), then were dropped synchronously together with NH₄HCO₃ solution, to a little amount of NH₄HCO₃ solution with initial pH = 9 under vigorous stirring, then the pH value was kept in the range of 8–9. The precipitate slurry was stirred sufficiently after the reaction. Then it was separated and was washed with deionized water for several times to remove NH₄⁺, NO₃⁻ and OH⁻, etc. The slurry cake was dried at 120 °C followed by repeated grinding. Finally, the dried precursor powders were sintered in the temperature range 800–1000 °C for 1 h.

The infrared (IR) spectra were recorded on a Fourier transform infrared spectrometer (Nicolet MAGNA-IR 750, USA). The phase development was characterized by Philips X'pert PRO x-ray diffractometer with Cu Kα₁ radiation. The morphology and microstructure of the sintered powders were observed by transmitted electron microscopy (Hitachi H-800, Japan). The photoluminescence spectra were measured using a Jobin-Yvon spectrophotometer (FLUOROLOG 3 TAU, France). All the experiments were completed at room temperature.

3. Results and discussion

Fig. 1 shows the XRD patterns of the precursor and the powders sintered for 1 h at various temperatures. No obvious diffraction peaks was observed for the precursor and the powder sintered at 800 °C, indicating that the samples are mainly amorphous. At 900 °C, strong characteristic diffraction peaks corresponding to cubic GSAG (JCPDS 43-0659) appeared. No other crystalline phase was observed, indicating the precursors transform into pure cubic

* Corresponding author. Tel.: +86 25 58731031; fax: +86 25 58731174.
E-mail address: zlj007@126.com (J. Su).

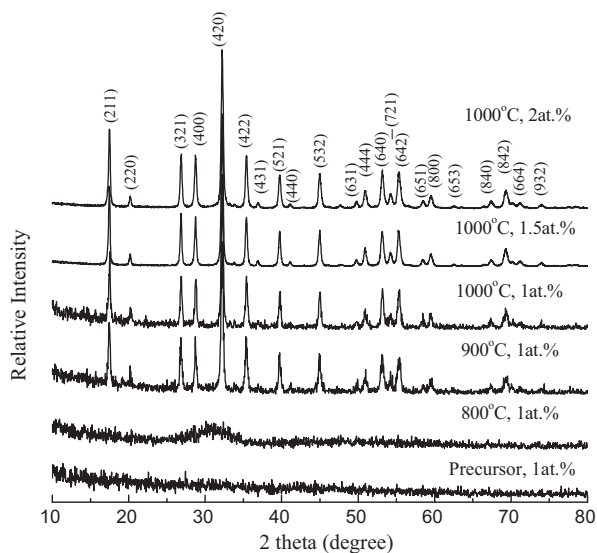


Fig. 1. X-ray diffraction patterns of the Nd:GSAG precursor and the samples sintered at different temperatures for 1 h.

GSAG polycrystalline. As the sintering temperature increases, the diffraction peaks became stronger and sharper, indicating the growth of Nd:GSAG crystallites. Additionally, the XRD pattern of Nd:GSAG polycrystalline with different Nd^{3+} concentration has no significant differences, indicating that at 2 at.% Nd^{3+} doping-level, the effect of doping Nd^{3+} on the crystal structure is unremarkable.

Fig. 2 shows the FT-IR spectra of the 1 at.% Nd^{3+} doped-precursor and the samples sintered at 800°C and 1000°C for 1 h, respectively. The wide bands at 3424 cm^{-1} can be assigned to O–H stretching modes of the crystal and absorbed water. The sharp band at 1386 cm^{-1} and the weak band around 1513 cm^{-1} are associated with NO_3^- , which became weaker with increasing of temperature due to the decomposition of NO_3^- . As raised to 800°C, the spectrum changed greatly because the structure of the precursor was destroyed. The new bands at 479 cm^{-1} and 744 cm^{-1} should be due to certain molecular modes of AlO_4 units [9], indicating the structure of the sample sintered at 800°C is not completely amorphous. For the sample sintered at 1000°C, new bands at 413 cm^{-1} , 475 cm^{-1} , 651 cm^{-1} , 679 cm^{-1} , 745 cm^{-1} appeared in the low frequency range of 800–400 cm^{-1} , which correspond to characteristic metal–oxygen (M–O) vibrations and can be attributed

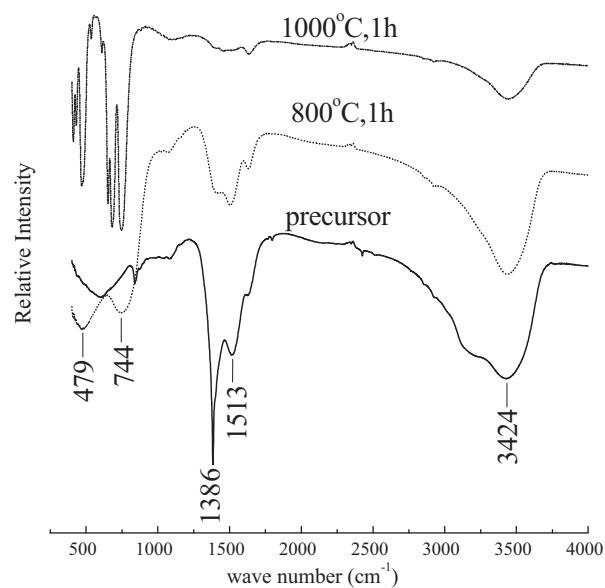


Fig. 2. FT-IR spectra of the Nd:GSAG precursor and the samples sintered at 800°C and 1000°C for 1 h.

to the stretching mode of the tetrahedral units present in garnet structure [10].

Fig. 3(a) and (b) shows TEM morphologies of the 2 at.% Nd:GSAG powders sintered at 900°C and 1000°C, respectively. Both the samples are well-dispersed with nearly spherical shape, and grand dimension of nanosizes (900°C, 30–60 nm; 1000°C, 50–80 nm). The average sizes of nanocrystallites could be determined from the broadening of diffraction lines of X-ray according to Scherer's formula ($d = 0.9\lambda / \beta \cos \theta$), and were estimated to be 37 and 50 nm for the samples sintered at 900°C and 1000°C, respectively. A slightly larger particle size observed in TEM micrographs than that in XRD patterns might be due to the resolution of instrumentation.

Fig. 4(a) shows the emission spectra of the Nd:GSAG samples sintered at 1000°C for 1 h. The spectra obtained by excitation in the $^4\text{I}_{9/2} \rightarrow ^4\text{F}_{5/2}$ transition of Nd^{3+} ion at 808 nm consist three main characteristic bands at 850–950, 1000–1150 and 1300–1380, which attribute to $^4\text{F}_{3/2} \rightarrow ^4\text{I}_{9/2}$, $^4\text{F}_{3/2} \rightarrow ^4\text{I}_{11/2}$, $^4\text{F}_{3/2} \rightarrow ^4\text{I}_{13/2}$ transition of Nd^{3+} , respectively. It shows that the emission peak at 1062 nm is most strong and the peak at 942 nm is relatively weak. Comparing the spectra of different Nd^{3+} concentration, no

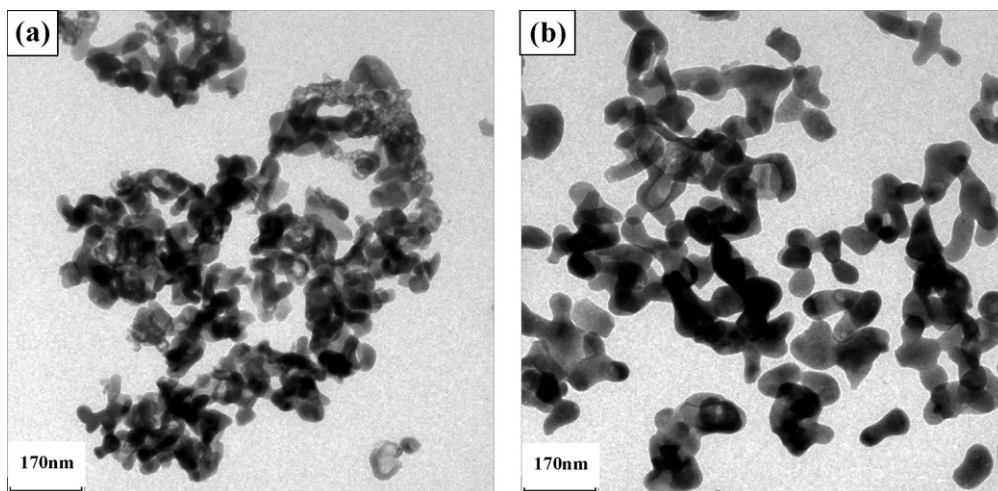


Fig. 3. TEM morphologies of Nd:GSAG samples sintered at 900°C (a) and 1000°C (b) for 1 h.

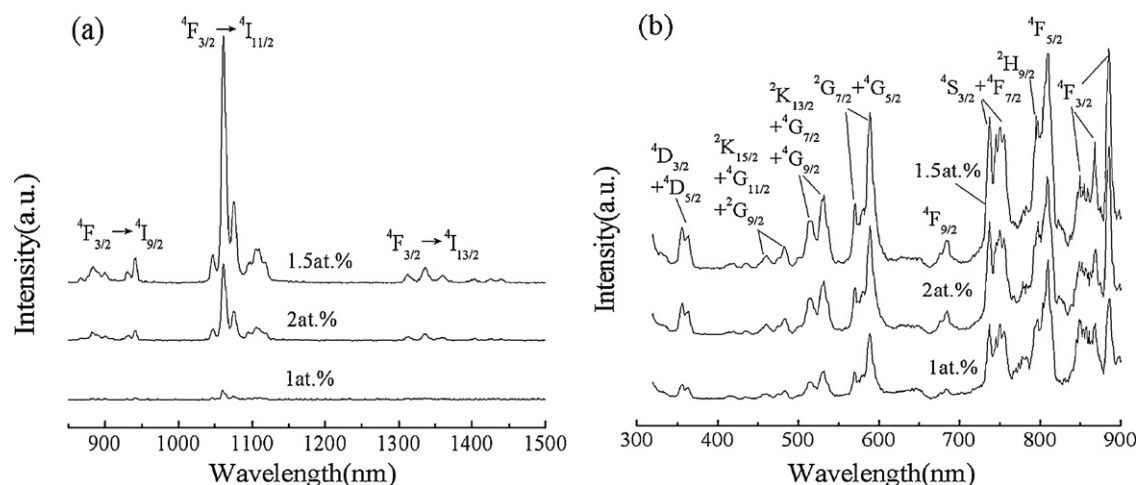


Fig. 4. Photoluminescence spectra of 1 at.%, 1.5 at.% and 2 at.% Nd:GSAG samples sintered at 1000 °C for 1 h: (a) emission spectra, $\lambda_{\text{ex}} = 808$ nm and (b) excitation spectra, $\lambda_{\text{em}} = 942$ nm.

significant difference in peak positions was found. The intensity at 1.5 at.% Nd-doped is strongest, while that of 2 at.% Nd-doped is decreased greatly, suggesting that concentration quenching of Nd^{3+} emission in GSAG observed is 1.5 at.%. As a suitable laser medium for quasi-three-level Nd^{3+} laser operation around 942 nm, Nd:GSAG crystal could be applied for atmospheric water vapor detection due to the fluorescence ratio of Nd^{3+} ${}^4\text{F}_{3/2} \rightarrow {}^4\text{I}_{9/2}$ is relatively large [11,12]. Thus we measured the excitation spectra monitored at 942 nm (${}^4\text{F}_{3/2} \rightarrow {}^4\text{I}_{9/2}$) of the Nd:GSAG nano-powders. According to the energy level of Nd^{3+} ion in GSAG [11–13], the excitation bands were assigned as Fig. 4(b) shows. It shows the intensities of the excitation bands changed significantly with the Nd^{3+} concentration, and the evolution of the intensities is the same as that shown in the emission spectra. The intensities of the excitation band at 808 nm are very strong, indicating the quasi-three-level Nd:GSAG laser transition at 942 nm could be operating by direct pumping with traditional pump of 808 nm LD.

4. Conclusions

Nd:GSAG precursors were co-precipitated from mixed nitrate solutions with NH_4HCO_3 as precipitant. Pure GSAG phase was obtained from sintering the precursors at 900 °C for 1 h. TEM and XRD results show that the precursor powders sintered at 900–1000 °C were well-dispersed with average crystalline sizes of 30–80 nm. The photoluminescence intensities of the nano-powders change significantly with the Nd^{3+} doping concentration and quenching concentration of Nd^{3+} in GSAG is about 1.5 at.%.

Acknowledgments

This work is supported by the National Natural Science Foundation of China (nos. 51002079 and 90922003).

References

- [1] R. Treichel, C. Czeranowsky, B. Ileri, K. Petermann, G. Huber, Proc. 5th ICSSO, 2004, pp. 639–642.
- [2] H. Rhee, T. Riesbeck, F. Kallmeyer, S. Strohmaier, H.J. Eichler, R. Treichel, K. Petermann, Proc. SPIE, vol. 6103, 2006, pp. 6103–6108.
- [3] S.G.P. Strohmaier, H.J. Eichler, C. Czeranowsky, B. Ileri, K. Petermann, G. Huber, Opt. Commun. 275 (2007) 170–172.
- [4] H.J. Eichler, F. Kallmeyer, H. Rhee, T. Riesbeck, S. Strohmaier, Proc. SPIE, vol. 6346, 2007, pp. 63460Y1–63460Y8.
- [5] A. Ikesue, T. Kinoshita, K. Kamata, K. Yoshida, J. Am. Ceram. Soc. 78 (1995) 1033–1040.
- [6] K. Takaichi, H. Yagi, J. Lu, A. Shirakawa, K. Ueda, T. Yanagitani, A.A. Kaminskii, Phys. Stat. Sol. A 200 (2003) R5–R7.
- [7] G. Qin, J. Lu, J.F. Bisson, Y. Feng, K. Ueda, H. Yagi, T. Yanagitani, Solid State Commun. 132 (2004) 103–106.
- [8] J. Lu, J. Lu, T. Murai, K. Takaichi, T. Uematsu, K. Ueda, H. Yagi, T. Yanagitani, A.A. Kaminskii, Jpn. J. Appl. Phys. 40 (2001) L1277–L1279.
- [9] K. Papagelis, G. Kanellis, S. Ves, G.A. Kourouklis, Phys. Stat. Sol. B 233 (2002) 134–150.
- [10] I. Mulioliene, S. Mathur, D. Jasaitis, H. Shen, V. Sivakov, R. Rapalaviciute, A. Beganskiene, A. Kareiva, Opt. Mater. 22 (2003) 241–250.
- [11] X. Jin, Q.L. Zhang, W.L. Zhou, X.L. Tan, W.P. Liu, S.T. Yin, H.H. Jiang, S.D. Xia, C.X. Guo, Acta Phys. Sin. 59 (2010) 7306–7313.
- [12] J. Su, B. Liu, L.H. Xu, Q.L. Zhang, S.T. Yin, J. Alloys Compd. 512 (2012) 230–234.
- [13] A.A. Kaminskii, Crystalline Lasers: Physical Processes and Operating Schemes, 1st ed., CRC Press, Boca Raton, 1996.